Mutual Coupling and Scattering Effects on Cellular CDMA Systems using Smart Antennas

Alexander M. Wyglinski and Steven D. Blostein
Queen's University at Kingston
Department of Electrical & Computer Engineering
Kingston, Ontario, Canada K7L 3N6
[alexw,sdb]@ee.queensu.ca

Abstract

It has been shown that CDMA systems which employ digital beamforming and base station antenna arrays potentially have significantly increased capacity. Therefore, methods are required to accurately predict the performance of these systems. One such method evaluates the system performance by studying the electromagnetic behavior of the base station antenna array. Unfortunately, in most studies using this method, the effects of mutual coupling in closely-spaced array elements as well as scattering due to multipath propagation are not considered, thus leading to potentially less accurate system performance predictions. In this paper, the development of an improved method where the effects of both mutual coupling and scattering are included in the system capacity predictions are presented and applied to system performance prediction.

1. Introduction

One of the primary restrictions for CDMA communication systems today is their susceptibility to interference from other co-channel users. Although several remedies have been proposed, CDMA systems which use digital beamforming and base station antenna arrays have been shown to be capable of achieving greater capacity relative to other multiple access techniques. This is possible since, from a collection of signals arriving at the antenna array, the desired signal can be isolated by multiplying the total signal received at the different array elements by a series of beamforming weights. These weights are chosen such that they co-phase the desired signal while randomizing the interfering signals.

One technique of predicting the performance of CDMA systems employing antenna arrays using digital beamforming is to study the electromagnetic behavior of the antenna array [3] [6] [11] [16]. Yet, many studies using this method do not consider the detrimental effects of mutual coupling and thus may potentially lead to less accurate system performance predictions. This problem can be avoided if information about the mutual coupling is somehow included in the system analysis.

The mutual coupling effects information may be extracted from an antenna array if it could be represented as an N-port network [2] [10] [8] [13] [16]. Thus, the circuit parameters associated with such a representation could be used to form a mutual impedance matrix, $[Z]$. Therefore, by using $[Z]$ in the derivation of the system capacity performance we are able to include the effects of mutual coupling and thus provide more accurate capacity predictions. Unfortunately, this may not be accurate enough unless the effects of a scatter environment are included as well.

The effects of scatter due to multipath propagation may be modeled by exploiting the second order statistics of the channel [1] [3] [9] [12]. Using these second order statistics, the resulting cross-correlation coefficients may be used in the analysis of the system capacity to yield accurate performance predictions.

In this paper, we present an improved method of determining the system capacity prediction by including both the effects of mutual coupling, using $[Z]$, and scatter due to multipath propagation, using the second order statistics. Thus, our resulting capacity predictions would potentially be more accurate relative to other results where one or both factors are neglected.

2 Mutual impedance information

To account for the effects of mutual coupling in our system performance predictions, we can use the following three methods, the induced EMF method, the method of moments, and a finite-element numerical computation, to represent the N_A-element antenna array as an N-port network. In this representation, the array is subdivided into N equal-length increments, each of which corresponds to a port. The goal of representing the array in this fashion is to exploit the associated circuit parameters, especially the driving-point impedances. These impedances can be organized into a mutual impedance matrix, $[Z]$, which contains the information on the mutual coupling effects of the array. Using $[Z]$, the mutual coupling effects information can be included in a beampattern synthesis formulation, as shown in [16], or a cell capacity prediction. It should be noted that the above three methods each have a distinct approach of obtaining $[Z]$, as described in the following three subsections.

2.1 Induced EMF method

Referring to [2], [10], and [16], the induced EMF method is a classical method of computing the self and mutual impedances of an N-port network representation of an antenna array. Although this method is restricted to straight, parallel, and in-echelon elements and does not account for the radius of the wires and the gaps at the feeds, its advantage is that it leads to closed-form solutions which provide adequate design data. Using the induced EMF method, we obtain the elements of $[Z]$, Z_{mn}, where $1 \leq m, n \leq N$, such that

$$Z_{mn} = \begin{cases} \begin{array}{c} 30\left(0.5772 + \ln(2\beta l) - Ci(2\beta l)\right) \\ +j30\left(Si(2\beta l)\right) \end{array} & , m = n \\ \\ R_{mn} + jX_{mn} & , m \neq n \end{cases} \tag{1}$$

where

$$\begin{gathered} R_{mn} = 30\cos(2\beta l)(Ci(u_0) + Ci(v_0) - 2Ci(u_1) \\ -2Ci(v_1) + 2Ci(\beta d)) + 30\sin(2\beta l)(-Si(u_0) \\ +Si(v_0) + 2Si(u_1) - 2Si(v_1)) \\ +30(-2Ci(u_1) - 2Ci(v_1) + 4Ci(\beta d)) \end{gathered}$$

$$\begin{gathered} X_{mn} = 30\cos(2\beta l)(-Si(u_0) - Si(v_0) + 2Si(u_1) \\ +2Si(v_1) - 2Si(\beta d)) + 30\sin(2\beta l)(-Ci(u_0) \\ +Ci(v_0) + 2Ci(u_1) - 2Ci(v_1)) \\ +30(2Si(u_1) + 2Si(v_1) - 4Si(\beta d)) \end{gathered}$$

$$\begin{array}{ll} u_0 = \beta(\sqrt{d^2 + 4l^2} - 2l) & v_0 = \beta(\sqrt{d^2 + 4l^2} + 2l) \\ u_1 = \beta(\sqrt{d^2 + l^2} - l) & v_1 = \beta(\sqrt{d^2 + l^2} + l) \\ Ci(u) = \int_{\infty}^{u} \frac{\cos(x)}{x} dx & Si(u) = \int_{0}^{u} \frac{\sin(x)}{x} dx \end{array}$$

and d is the horizontal distance between two dipole antennas, l is half the length of the dipole antenna, and β is the wave number, namely, $\beta = 2\pi/\lambda$. It should be noted that in this derivation, we let $N = N_A$.

As mentioned in [16], $[Z]$ may be used in beampattern synthesis to account for the effects of mutual coupling within the beampatterns. Doing so requires solving the matrix equation $[Z]^{-1}\overrightarrow{V} = \overrightarrow{I}$, where $\overrightarrow{V}$ is a vector of the voltages along each antenna, $\overrightarrow{I}$ is a vector of the currents along each antenna, and $[Z]^{-1}$ is the inverse matrix of $[Z]$. Defining $\overrightarrow{V}$, the currents over the array can be determined. Once $\overrightarrow{I}$ is found, beampattern synthesis is performed using

$$A(\theta) = \left| \sum_{m=1}^{N_A} I_m e^{j\left(\frac{\pi\cos(\theta - m(2\pi/N_A))}{2\sin(\pi/N_A)}\right)} \right|^2 \tag{2}$$

where I_m is an element of $\overrightarrow{I}$, θ is the AOA (angle-of-arrival), and N_A is the number of antenna elements.

A sample beampattern which includes mutual coupling effects generated using the induced EMF method is shown in Figure 4. A comparison of beampatterns using mutual coupling information generated by various methods is performed in Section 5.

2.2 Method of moments

The method of moments is another technique of obtaining the mutual impedance matrix $[Z]$, as described in [8] [13]. Using basic equations from electromagnetics and assuming that the current flows in one direction, the current and charge densities are approximated by filaments of current and charge on the wire axis, and viewing the antenna array as a system of N small increments which constitute an N-port network. Thus, an element of the mutual impedance matrix $[Z]$, Z_{mn}, where $1 \leq m, n \leq N$, is given by

$$\begin{gathered} Z_{mn} = j\omega\mu\Delta\vec{l}_n \cdot \Delta\vec{l}_m \psi(n,m) + \tfrac{1}{j\omega\varepsilon}[\psi(n^+, m^+) \\ -\psi(n^-, m^+) - \psi(n^+, m^-) + \psi(n^-, m^-)] \end{gathered} \tag{3}$$

$$\psi(n,m) = \frac{1}{\Delta l_n} \int_{\Delta l_n} \frac{e^{-jkR_m}}{4\pi R_m} dl \tag{4}$$

$$R_m = \begin{cases} \sqrt{\rho^2 + (z - z_m)^2} & , \quad m \neq n \\ \sqrt{a^2 + z^2} & , \quad m = n \end{cases} \tag{5}$$

where ρ is the horizontal distance between antennas containing points n and m, a is the dipole antenna radius, k is the wave number, z_m is the vertical distance between points n and m, μ is the permeability, ϵ is the permittivity, Δl_n is the length of the n^{th} increment, ω is the frequency of operation (in radians per second), n^- and n^+ denote the starting and terminating points of the n^{th} increment, and m^- and m^+ denote the starting and terminating points of the m^{th} increment.

To perform beampattern synthesis, we numerically integrate $\psi(n,m)$, thus obtaining $[Z]$ which is then used to solve $[Z]^{-1}\overrightarrow{V} = \overrightarrow{I}$, where $\overrightarrow{V}$ specifies a vector of the increment voltages and $\overrightarrow{I}$ specifies a vector of the increment currents. If the antennas are center-fed, only the increments corresponding to the centers of the antennas will have a nonzero voltage. Upon obtaining $\overrightarrow{I}$, we perform beampattern synthesis by determining the far-zone field at a point i using [13]

$$A_i = \frac{\mu e^{-jkr_i}}{4\pi r_i}\sum_{j=1}^{n} I_j e^{jkr_j \cos\xi_{ij}}\Delta l_j \tag{6}$$

where r_i and r_j are the radius vectors to the distant field and source points, respectively, and ξ_{ij} is the angle between them.

A sample beampattern which includes mutual coupling effects generated using the method of moments is shown in Figure 5.

2.3 Finite-element numerical computation

In this study, we use a finite-element numerical computation software package known as IE3D [17]. It is capable of modeling both the electric current on a metallic structure as well as a magnetic current representing the field distribution on a metallic aperture.

The computation process of IE3D is based upon solving an integral equation derived using green's functions and the method of moments [17]. An element of the $N \times N$ mutual impedance matrix $[Z]$, Z_{mn}, is given as

$$Z_{mn} = \int_S \{Z_s \vec{B_m}\cdot\vec{B_n}\}ds + \int_S ds \int_S \{\vec{B_m}\cdot\vec{G}(\vec{r}|\vec{r'})\cdot\vec{B_n}\}ds' \tag{7}$$

where Z_s is the surface impedance of the conductor, $\vec{B_n}(\vec{r})$ is a basis function, and $\vec{G}(\vec{r}|\vec{r'})$ is a green's function.

In order to perform beampattern synthesis, IE3D uses Equation (7) and solves for the current distribution across the array using

$$V_n = \int_S \{\vec{E_i}(\vec{r})\cdot\vec{B_n}\}ds \tag{8}$$

and

$$[Z]\overrightarrow{I} = \overrightarrow{V} \tag{9}$$

where the voltage vector $\overrightarrow{V}$ and mutual impedance matrix $[Z]$ are computed and use (9) to solve for the current vector $\overrightarrow{I}$. A sample beampattern generated using IE3D is shown in Figure 6.

It should be noted that the differences among finite elements formulations are based on the choice of $\vec{B_n}(\vec{r})$ for the current distribution representation and $\vec{G}(\vec{r}|\vec{r'})$.

3 Scatter

Scatter is a phenomenon associated with multipath propagation. It occurs when signals from a single source arrive at a base station from several directions within an angular region after being reflected by objects in the surrounding environment. This angular region, known as the *angle spread*, varies according to the operating environment.

In this section, the modified cross-correlation statistics for a multipath fading channel, where mutual coupling effects are included, is presented. Using these statistics, the cell capacity of a system operating within a scatter environment which includes the effects of mutual coupling can be determined.

3.1 Cross-correlation statistics

Derivations of the cross-correlation statistics of the multipath fading channel may be found in [1], [3], [11], and [12]. Yet, unlike those derivations, ours goes one step further by also including the antenna array mutual coupling effects. Furthermore, we assumed that there is no specific distribution used such that the resulting analysis could be applied to a variety of cases.

Assuming we have two identical antennas, i and k, that are spaced a distance d apart receiving signals from the same source, the total voltages produced by all the waves at antennas i and k, where the r^{th} wave makes an angle θ_{k_r} with a line passing through antennas i and k, is

$$\begin{aligned} v_i &= \sum_{r=1}^{n} a_r \cos\left(\omega t + \psi_r + \frac{\pi d}{\lambda}\cos(\theta_{k_r})\right) \\ &= A_1 \cos(\omega t + \Psi_1) \end{aligned} \tag{10}$$

$$\begin{aligned} v_k &= \sum_{r=1}^{n} a_r \cos\left(\omega t + \psi_r - \frac{\pi d}{\lambda}\cos(\theta_{k_r})\right) \\ &= A_2 \cos(\omega t + \Psi_2) \end{aligned} \tag{11}$$

with frequency $f = \omega/2\pi$ and wavelength λ. The phase delay of the ray r is represented by the value ψ_r while the amplitude of the ray r is defined as a_r. The amplitudes and phases are generally different at the two antennas. Furthermore, the voltages at antennas i and k are zero mean while the mean squared amplitude is

$$\overline{A_1^2} = \overline{A_2^2} = \sum_{r=1}^{n} a_r^2 \tag{12}$$

Suppose a distribution of waves is assumed, then given a distribution of arriving signal power, $P(\theta)$, the total power received from the whole distribution of waves is

$$P_o = \int_0^{2\pi} P(\theta)d\theta \tag{13}$$

and Equation (12) becomes

$$\overline{A_1^2} = \overline{A_2^2} = 2P_o = 2\int_0^{2\pi} P(\theta)d\theta \qquad (14)$$

To include the effects of mutual coupling, we must multiply Equations (10) and (11) by an admittance matrix $[Y]$, which is the inverse of the mutual impedance matrix $[Z]$ generated using the induced EMF method, thus yielding

$$\begin{aligned} v_{i,mc} &= |Y_{ii}|\, A_1 \cos(\omega t + \Psi_1)\, e^{j\angle Y_{ii}} \\ &+ |Y_{ik}|\, A_2 \cos(\omega t + \Psi_2)\, e^{j\angle Y_{ik}} \\ &= B_{1c}\cos(\omega t) + B_{1s}\sin(\omega t) \qquad (15) \end{aligned}$$

$$\begin{aligned} v_{k,mc} &= |Y_{ki}|\, A_1 \cos(\omega t + \Psi_1)\, e^{j\angle Y_{ki}} \\ &+ |Y_{kk}|\, A_2 \cos(\omega t + \Psi_2)\, e^{j\angle Y_{kk}} \\ &= B_{2c}\cos(\omega t) + B_{2s}\sin(\omega t) \qquad (16) \end{aligned}$$

where, for example, $|Y_{ik}|$ and $\angle Y_{ik}$ represent the magnitude and phase of the mutual admittance between antenna elements i and k, respectively.

Since the phase angles ψ_r are assumed to be random and n is assumed to be large, we can model B_{1c}, B_{1s}, B_{2c}, and B_{2s} as distributed normally with zero mean.

To determine the joint probability distribution of A_1 and A_2, their second moments, $\overline{B_{1c}^2}$, $\overline{B_{1s}^2}$, $\overline{B_{2c}^2}$, $\overline{B_{2s}^2}$, $\overline{B_{1c}B_{2c}}$, $\overline{B_{1s}B_{2s}}$, $\overline{B_{1c}B_{1s}}$, $\overline{B_{2c}B_{2s}}$, $\overline{B_{1c}B_{2s}}$, and $\overline{B_{2c}B_{1s}}$, must be obtained, where $\overline{(.)}$ is the expectation of $(.)$. For further simplification, since the admittance matrix is symmetric, we allowed $\angle Y_{ii} = \angle Y_{kk}$, $\angle Y_{ik} = \angle Y_{ki}$, $|Y_{ii}| = |Y_{kk}|$, and $|Y_{ik}| = |Y_{ki}|$. Therefore, after extensive derivations using Equations (14), (15), and (16), we obtain the generalized cross-correlation coefficients [15]

$$\begin{aligned} b_o &= \overline{B_{1c}^2} = \overline{B_{1s}^2} = \overline{B_{2c}^2} = \overline{B_{2s}^2} \\ &= \left(|Y_{ii}|^2 + |Y_{ik}|^2\right) \int_0^{2\pi} P(\theta)d\theta \\ &+ 2|Y_{ii}||Y_{ki}|\cos(\angle Y_{ii} - \angle Y_{ki}) \\ &\quad \cdot \int_0^{2\pi} P(\theta)\cos\left(\frac{2\pi d}{\lambda}\cos(\theta)\right)d\theta \qquad (17) \end{aligned}$$

$$\begin{aligned} \rho_{R_iR_k} &= \overline{B_{1c}B_{2c}} = \overline{B_{1s}B_{2s}} \\ &= 2|Y_{ii}||Y_{ki}| \int_0^{2\pi} P(\theta)\cos(\angle Y_{ii} - \angle Y_{ki})d\theta \\ &+ \left(|Y_{ii}|^2 + |Y_{ik}|^2\right) \\ &\quad \cdot \int_0^{2\pi} P(\theta)\cos\left(\frac{2\pi d}{\lambda}\cos(\theta)\right)d\theta \qquad (18) \end{aligned}$$

$$\begin{aligned} \rho_{R_iI_k} &= \overline{B_{1c}B_{2s}} = -\overline{B_{2c}B_{1s}} \\ &= -\left(|Y_{ii}|^2 - |Y_{ik}|^2\right) \\ &\quad \cdot \int_0^{2\pi} P(\theta)\sin\left(\frac{2\pi d}{\lambda}\cos(\theta)\right)d\theta \qquad (19) \end{aligned}$$

$$\overline{B_{1c}B_{1s}} = \overline{B_{2c}B_{2s}} = 0 \qquad (20)$$

where $\rho_{R_iR_k}$ is the cross-correlation factor of the real component of the Rayleigh fading value at antenna element i with the real component of the Rayleigh fading value at antenna element k, $\rho_{R_iI_k}$ is the cross-correlation factor of the real component of the Rayleigh fading value at antenna i with the imaginary component of the Rayleigh fading value at element j, and b_o is the mean squared of B_{1c}, B_{1s}, B_{2c}, and B_{2s}.

Suppose we specify a Gaussian $P(\theta)$ with mean θ_d and variance equivalent to that of a uniform distribution over $[\theta_d - \Delta, \theta_d + \Delta]$ is defined as

$$P(\theta) = \frac{1}{\sqrt{2\pi\sigma_\Delta^2}} e^{\frac{-(\theta-\theta_k)^2}{2\sigma_\Delta^2}} \qquad (21)$$

where $\sigma_\Delta^2 = \frac{\Delta^2}{3}$, then Equations (17), (18), and (19) become

$$\begin{aligned} b_o &= \left(|Y_{ii}|^2 + |Y_{ik}|^2\right) \\ &\quad \cdot \left(erf\left(\frac{2\pi - \theta_k}{\sigma_\Delta}\right) + erf\left(\frac{\theta_k}{\sigma_\Delta}\right)\right) \\ &+ 2|Y_{ii}||Y_{ki}|\cos(\angle Y_{ii} - \angle Y_{ki}) \left(J_o\left(\frac{2\pi d}{\lambda}\right)\right. \\ &+ \left. 2\sum_{m=1}^{\infty} J_{2m}\left(\frac{2\pi d}{\lambda}\right)\cos(2m\theta_k)\, e^{-2m^2\sigma_\Delta^2}\right) \end{aligned} \qquad (22)$$

$$\begin{aligned} \rho_{R_iR_k} &= 2|Y_{ii}||Y_{ki}|\cos(\angle Y_{ii} - \angle Y_{ki}) \\ &\quad \cdot \left(erf\left(\frac{2\pi - \theta_k}{\sigma_\Delta}\right) + erf\left(\frac{\theta_k}{\sigma_\Delta}\right)\right) \\ &+ \left(|Y_{ii}|^2 + |Y_{ik}|^2\right) \left(J_o\left(\frac{2\pi d}{\lambda}\right)\right. \\ &+ \left. 2\sum_{m=1}^{\infty} J_{2m}\left(\frac{2\pi d}{\lambda}\right)\cos(2m\theta_k)\, e^{-2m^2\sigma_\Delta^2}\right) \end{aligned} \qquad (23)$$

$$\begin{aligned} \rho_{R_iI_k} &= -\left(|Y_{ii}|^2 - |Y_{ik}|^2\right) \left(2\sum_{m=1}^{\infty} J_{2m+1}\left(\frac{2\pi d}{\lambda}\right)\right. \\ &\quad \cdot \left. \sin((2m+1)\,\theta_k)\, e^{\frac{-(2m+1)^2\sigma_\Delta^2}{2}}\right) \qquad (24) \end{aligned}$$

where $erf(x)$ is

$$erf(x) = \frac{2}{\sqrt{\pi}} \int_0^x e^{-t^2} dt \qquad (25)$$

4 Cell capacity estimation

The system under analysis assumes perfect power control in a single cell environment where the base station antenna array consists of N_A antennas.

According to [7] and [14], for a single cell that contains N_M mobiles, there exists one desired mobile, with received signal power P_R, and $N_M - 1$ interfering mobiles, each with received signal power P_{I_k}. Assuming that the voice activity factor α is unity and all the reverse link signals are received at the same signal power, the bit energy-to-noise density ratio is

$$\frac{E_b}{N_o} = \frac{P_R/R_B}{P_I/B + N_A\sigma_n^2} \tag{26}$$

where σ_n^2 is the variance of the background noise, R_B is the data bit rate, and B is the bandwidth of the spreaded signal.

Replacing P_R with $E\left\{\phi_d\right\} P_R$ and P_I with $E\left\{\phi_k\right\} P_R N_I$, where N_I is the number of interfering mobiles, Equation (26) becomes

$$\frac{E_b}{N_o} = \frac{E\left\{\phi_d\right\} P_R/R_B}{E\left\{\phi_k\right\} P_R N_I/B + N_A\sigma_n^2} \tag{27}$$

and solving for P_R yields

$$P_R = N_A\sigma_n^2\left(\frac{E_b}{N_o}\right)\left\{\frac{E\{\phi_d\}}{R_B} - \frac{E\{\phi_k\}N_I}{B}\left(\frac{E_b}{N_o}\right)\right\}^{-1} \tag{28}$$

which can then yield the system capacity by finding the maximum value of $N_M = N_I + 1$ which make Equation (28) zero. Thus, we obtain

$$N_M = N_I + 1 = \left\lfloor \frac{1}{E\left\{\phi_k\right\}}\frac{E\left\{\phi_d\right\} B}{R\left(\frac{E_b}{N_o}\right)}\right\rfloor + 1 \tag{29}$$

4.1 Determining $E\{\phi_k\}$ and $E\{\phi_d\}$

We can determine the expected interference and mobile power, $E\{\phi_k\}$ and $E\{\phi_d\}$, respectively, in a scattering environment using correlation statistics in Section 3.1 where the effects of mutual coupling are included.

Assuming that maximum SNR beamforming is performed for a circular array geometry, the array response vector, $\bar{a}(\theta)$, and the beamforming weight vector, $\bar{\omega}(\theta)$, are

$$\bar{a}(\theta) = \bar{\omega}(\theta) = \begin{bmatrix} e^{j\alpha_0(\theta)} \\ e^{j\alpha_1(\theta)} \\ e^{j\alpha_2(\theta)} \\ \vdots \\ e^{j\alpha_{(N_A-1)}(\theta)} \end{bmatrix} \tag{30}$$

where the phase delay for ith element of the array, $\alpha_i(\theta)$, is given by

$$\alpha_i\left(\theta\right) = \pi\cos\left(\theta - i\frac{2\pi}{N_A}\right)/2\sin\left(\frac{\pi}{N_A}\right) \tag{31}$$

It should be noted that these beamforming weights can be reconfigured to other array geometries as well.

Therefore, to include the mutual coupling effects in our analysis, our modified beamforming weight vector, $\bar{\omega}_{MC}$, is

$$\bar{\omega}_{MC}\left(\theta_d\right) = [Z]^{-1}\bar{\omega}\left(\theta_d\right) = [Y]\bar{\omega}\left(\theta_d\right) \tag{32}$$

where $[Z]^{-1}$ is the matrix inverse of $[Z]$, $[Y]$ is equal to $[Z]^{-1}$, $[Y]$ and $[Z]$ are $N_A \times N_A$ matrices where N_A is the number of array elements, and θ_d is the mean angle-of-arrival for the desired user.

Furthermore, to account for the received signal strength due to mobile k at element i, β_{ki}, our modified array response vector, $\bar{a}_\beta$, is

$$\begin{aligned} \bar{a}_\beta\left(\theta_k\right) &= [\beta]\bar{a}\left(\theta_k\right) \\ &= \begin{bmatrix} \beta_{k1} & 0 & \cdots & 0 \\ 0 & \beta_{k2} & & \vdots \\ \vdots & & \ddots & 0 \\ 0 & \cdots & 0 & \beta_{kN_A} \end{bmatrix} \bar{a}\left(\theta_k\right) \end{aligned} \tag{33}$$

where $[\beta]$ is the $N_A \times N_A$ received signal strength matrix whose diagonal elements correspond to values of β_{ki}, and θ_k is the mean angle-of-arrival for a mobile k.

Using Equations (32) and (33), the normalized amount of interference power seen from an interferer k at an angle-of-arrival θ_k is

$$\phi_k\left(\theta_d, \theta_k\right) = \left|\frac{\bar{\omega}_{MC}^{\mathbf{H}}\left(\theta_d\right)}{\left\|\bar{\omega}_{MC}^{\mathbf{H}}\left(\theta_d\right)\right\|}\frac{\bar{a}_\beta\left(\theta_k\right)}{\left\|\bar{a}_\beta\left(\theta_k\right)\right\|}\right|^2 \tag{34}$$

where $\bar{\omega}_{MC}^{\mathbf{H}}\left(\theta_d\right)$ denotes the complex conjugate transpose of $\bar{\omega}_{MC}\left(\theta_d\right)$ and $\|.\|$ is the vector norm.

Since β_{ki} is proportional to a Rayleigh fading random variable for mobile k at array element i, extensive manipulation of Equation (34) has been carried out in order to attain a usable form. Thus, by letting $\beta_{ki} = \eta_k R_{ki}$ and assuming that both θ_k and θ_d are random variables uniformly distributed over $[0^o, 360^o)$, the expected values of $\left|\bar{\omega}_{MC}^{\mathbf{H}}\left(\theta_d\right)\bar{a}_\beta\left(\theta_k\right)\right|^2$ and $\left\|\bar{a}_\beta\left(\theta_k\right)\right\|^2$ in Equation (34) conditioned on θ_k, θ_d, and σ_Δ^2 can be shown to be [15]

$$\begin{aligned} &E\left\{\left|\bar{\omega}_{MC}^{\mathbf{H}}\left(\theta_d\right)\bar{a}_\beta\left(\theta_k\right)\right|^2\middle|\,\theta_k, \theta_d, \sigma_\Delta^2\right\} \\ &= E\left\{\sum_{i=1}^{N_A}\sum_{l=1}^{N_A}\sum_{p=1}^{N_A}\sum_{r=1}^{N_A}\eta_k^2 R_{ki}R_{kr}Y_{li}^{*}Y_{rp}\chi_{ilpr}\,\middle|\,\theta_k, \theta_d, \sigma_\Delta^2\right\} \end{aligned}$$

$$= E\left\{\eta_k^2\right\} \sum_{i=1}^{N_A} \sum_{l=1}^{N_A} \sum_{p=1}^{N_A} \sum_{r=1}^{N_A} E\left\{ R_{ki} R_{kr} \middle| \sigma_\Delta^2 \right\} Y_{li}^* Y_{rp} \chi_{ilpr} \tag{35}$$

$$E\left\{ \left\|\bar{a}_\beta\left(\theta_k\right)\right\|^2 \middle| \theta_k, \theta_d, \sigma_\Delta^2 \right\} = E\left\{ \sum_{i=1}^{N_A} \eta_k^2 R_{ki}^2 \middle| \theta_k, \theta_d, \sigma_\Delta^2 \right\}$$
$$= E\left\{\eta_k^2\right\} \sum_{i=1}^{N_A} E\left\{ R_{ki}^2 \middle| \sigma_\Delta^2 \right\} \tag{36}$$

where σ_Δ^2 is the variance of the spatial angle-of-arrival (AOA) distribution $P(\theta)$, $\chi_{ilpr} = e^{j(\alpha_i + \alpha_p - \alpha_r - \alpha_l)}$ such that α_i, α_l, α_p, and α_r are defined by Equation (31), η_k is the path loss and shadowing effects factor at mobile k, and R_{ki} is the Rayleigh fading random variables for mobile k at array element i. We assumed that the factor η_k is independent of R_{ki} and is equal across the antenna array.

Furthermore, Davenport and Root in [4] have shown that $E\{R_{ki}R_{kj}\}$, the cross-correlation between the Rayleigh distributed random variables at antennas i and j due to mobile k, can be given in terms of the confluent hypergeometric function ${}_2F_1\left(-\frac{1}{2}, -\frac{1}{2}; 1; .\right)$ yielding

$$E\{R_{ki}R_{kj}\} = \frac{\pi}{2} b_o \left({}_2F_1\left(-\frac{1}{2}, -\frac{1}{2}; 1; \zeta_{ji}^2\right)\right) \tag{37}$$

where $\zeta_{ji}^2 = \left(\rho_{R_iR_j}^2 + \rho_{R_iI_j}^2\right)/b_o^2$. Therefore, using Equation (37), (35), and (36), Equation (34) can be rewritten as

$$\phi_k\left(\theta_d, \theta_k\right) = \left(2N_A \sum_{h=1}^{N_A} \sum_{s=1}^{N_A} \sum_{m=1}^{N_A} e^{j(\alpha_h - \alpha_s)} Y_{sm}^* Y_{mh}\right)^{-1}$$
$$\cdot \frac{\pi}{2} b_o \sum_{i=1}^{N_A} \sum_{l=1}^{N_A} \sum_{p=1}^{N_A} \sum_{r=1}^{N_A} {}_2F_1\left(-\frac{1}{2}, -\frac{1}{2}; 1; \zeta_{ji}^2\right) Y_{li}^* Y_{rp} \chi_{ilpr} \tag{38}$$

Once $\phi_k\left(\theta_d, \theta_k\right)$ is obtained, we then proceed to determine $E\left\{\phi_k\right\}$. Uniformly averaging Equation (38) over θ_k and θ_d yields

$$E\left\{\phi_k\right\} = \frac{1}{N_\theta^2} \sum_{\theta_d \in \Theta_d} \sum_{\theta_k \in \Theta_k} \phi_k\left(\theta_k, \theta_d\right) \tag{39}$$

where Θ_k and Θ_d are sets of N_θ angle-of-arrivals that range uniformly over $[0^o, 360^o)$.

Similarly, due to the fact that some of the desired signal will be suppressed because not all of the signal is located at the maximum of the spatial filter corresponding to the maximum SNR beamformer, the expected percentage of the desired signal being passed by the beamforming pattern for a mean angle-of-arrival θ_d must be determined for an unspecified spatial distribution of the incoming signal, $P(\theta)$. This may be accomplished by averaging Equation (38) uniformly over θ_d and θ, yielding

$$E\left\{\phi_d\right\} = \frac{2\pi}{N_\theta^2} \sum_{\theta_d \in \Theta_d} \sum_{\theta \in \Theta} P(\theta) \phi_k\left(\theta, \theta_d\right) \tag{40}$$

where Θ and Θ_d range uniformly over $[0^o, 360^o)$.

Suppose, for example, we use a Gaussian $P(\theta)$ with mean θ_d and variance equivalent to that of a uniform distribution over $[\theta_d - \Delta, \theta_d + \Delta]$, as defined in Equation (21). Then, by using Equation (40), the expected percentage of the desired signal being passed by the beamforming pattern is

$$E\left\{\phi_d\right\} = \frac{\sqrt{6\pi}}{N_\theta^2} \frac{1}{|\Delta|} \sum_{\theta_d \in \Theta_d} \sum_{\theta \in \Theta} e^{-\frac{3(\theta - \theta_d)^2}{2\Delta^2}} \phi_k\left(\theta, \theta_d\right) \tag{41}$$

Therefore, using numerical computation, $E\left\{\phi_d\right\}$ and $E\left\{\phi_k\right\}$ can determined and used in Equation (29).

5 Results

Figures 1 and 2 are the result of Equation (29) for a Gaussian angle-of-arrival (GAA) spatial distribution. From them, it is evident that the effects of mutual coupling, in conjunction with a scattering environment, deteriorates the system's performance significantly. Furthermore, when angle spread is small, the deteriorating effects of mutual coupling are prevalent. Yet, when the angle spread increases, the effects of scattering become the dominant deteriorating factor and eventually all the curves converge to the single antenna case.

Beampattern synthesis allows us to visualize the detrimental impact of mutual coupling effects on system performance. Referring to the normalized beampatterns of Figures 3-6, resulting from a 4-element circular array consisting of half-wavelength dipoles with AOA of 45^o, we make the following observations: (1) comparing Figure 3, where mutual coupling effects are not included, with Figures 4-6, which do include these effects, it is observed that Figures 4-6 all exhibit higher sidelobe levels, shallower nulls, and wider beamwidths relative to Figure 3. (2) Figures 4-6 all agree closely with one another. Therefore, finite element numerical computations could be used to predict beampatterns of larger classes of antenna arrays which cannot be analytically studied, including directional antennas.

6 Conclusion

From our improved method for predicting the capacity of a CDMA system which employs base station antenna arrays and uses digital beamforming, we see that both the effects of mutual coupling and scatter due to multipath degrade the performance of the system. Specifically, the mutual coupling effects are dominant when angle spread is relatively small and the numbers of antennas is large. Scattering effects, on the other hand, are dominant for large angle spread. Moreover, the capacity of the system with multiple antennas converges to the single antenna element case when the angle spread increases.

7 Future work

Currently, we are investigating an improved system capacity prediction where imperfect power control is assumed. Using an approach in [14], the SNR is a random variable with a log-normal distribution, rather than a fixed value when using the perfect power control assumption. Moreover, an outage probability exists when a threshold SNR is specified.

References

[1] E. N. Bramley. Diversity effects in spaced-aerial reception of ionospheric waves. *IEE Proceedings*, 98(3):19–25, 1951.

[2] P. S. Carter. Circuit relations in radiating systems and applications to antenna problems. *Proceedings of the IEEE*, 20(6):1004–1041, June 1932.

[3] G. W. K. Colman. An investigation into the capacity of cellular cdma commnications systems with beamforming in environments with scatter. Master's thesis, Queen's University at Kingston, 1998.

[4] W. B. Davenport, Jr. and W. L. Root. *An Introduction to the Theory of Random Signals and Noise*. McGraw-Hill, Inc., 1994.

[5] J. F. Diouris, S. McLaughlin, and J. Zeidler. Sensitivity analysis of the performance of a diversity receiver. *1999 IEEE International Conference on Communications*, 1999.

[6] A. M. Earnshaw and S. D. Blostein. Efficient evaluation of adaptive digital beamforming for multi-service provision in a cellular cdma system. *48th IEEE Vehicular Technology Conference*, 1998.

[7] K. S. Gilhousen, I. M. Jacobs, R. Padovani, A. J. Viterbi, L. A. Weaver, and C. E. Wheatley III. On the capacity of a cellular cdma system. *IEEE Transactions on Vehicular Technology*, 40(2):303–312, May 1991.

[8] R. F. Harrington. *Field Computation by Moment Method*. MacMillan Co., 1968.

[9] W. C. Jakes. *Mobile Microwave Communications*. John Wiley and Sons, 1974.

[10] H. E. King. Mutual impedance of unequal length antennas in echelon. *IRE Transactions on Antennas and Propagation*, 5:306–313, July 1957.

[11] A. F. Naguib. *Adaptive Antennas for CDMA Wireless Networks*. PhD thesis, Stanford University, 1995.

[12] J. Salz and J. H. Winters. Effect of fading correlation on adaptive arrays in digital mobile radio. *IEEE Transactions on Vehicular Technology*, 43(4):1049–1057, 1994.

[13] B. T. Strait and A. T. Adams. Analysis and design of wire antennas with applications to emc. *IEEE Transactions on Electromagnetic Compatibility*, 12(2):45–54, May 1970.

[14] A. J. Viterbi. *CDMA: Principles of Spread Spectrum Communication*. Addison-Wesley, 1995.

[15] A. M. Wyglinski. Performance of cdma systems using digital beamforming with mutual coupling and scattering effects. Master's thesis, Queen's University at Kingston, 2000.

[16] A. M. Wyglinski and S. D. Blostein. Antenna array mutual coupling effects on cellular cdma communication systems. *Proc. 20th Biennial Symposium on Communications*, 2000.

[17] Zeland. *IE3D Electromagnetic Simulator: User Manual*. Zeland Software Inc., 5rd edition, 1999.

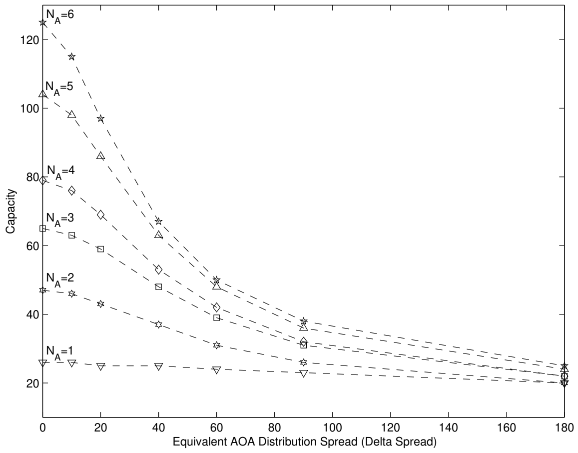

Figure 1. Capacity predictions of a GAA spatial distribution without mutual coupling effects

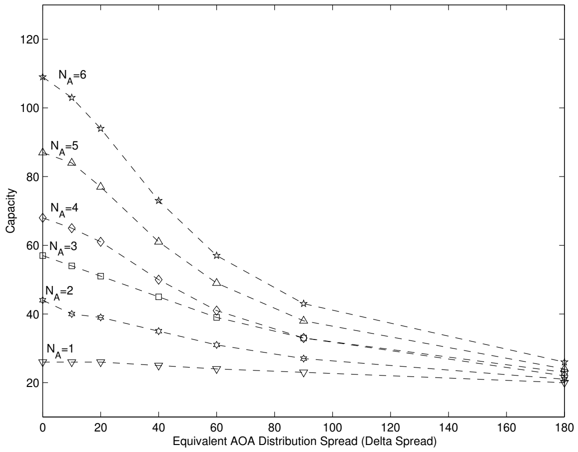

Figure 2. Capacity predictions of a GAA spatial distribution with mutual coupling effects

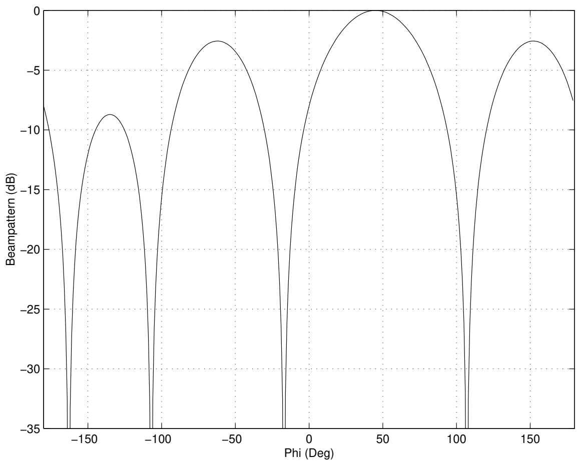

Figure 3. Beampattern with AOA of 45^o for a 4-element circular array without mutual coupling effects

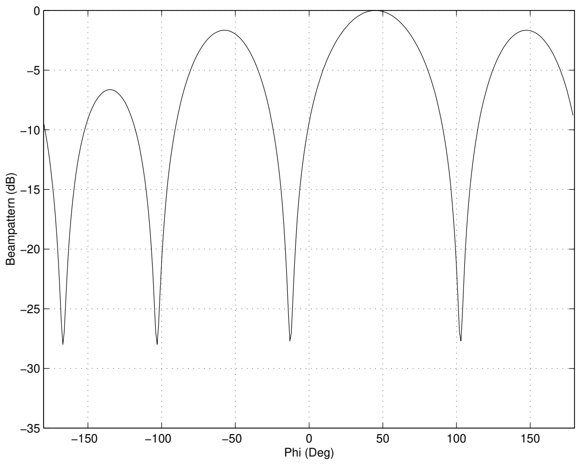

Figure 4. Beampattern with AOA of 45^o for a 4-element circular array with induced EMF method-generated mutual coupling effects

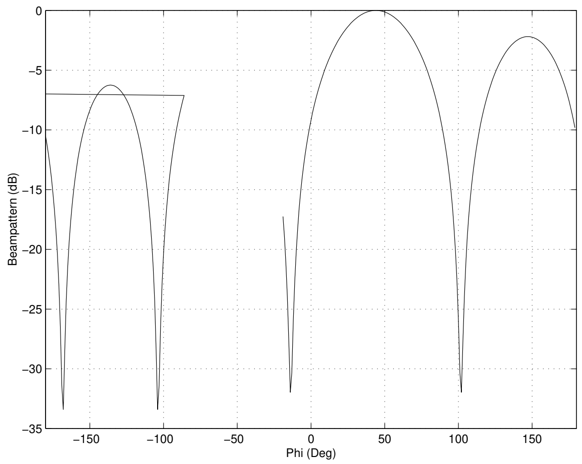

Figure 5. Beampattern with AOA of 45^o for a 4-element circular array with method of moments-generated mutual coupling effects

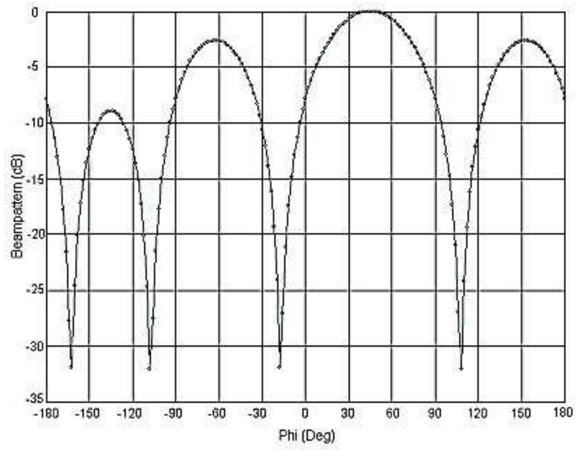

Figure 6. Beampattern with AOA of 45^o for a 4-element circular array with finite-element numerical computation-generated mutual coupling effects